Utility of ^{18}F-Fluciclovine PET/MRI for Staging Newly Diagnosed High-Risk Prostate Cancer and Evaluating Response to Initial Androgen Deprivation Therapy: A Prospective Single-Arm Pilot Study

Samuel J. Galgano, MD[1,2], **Andrew M. McDonald, MD, MS**[2,3,4], **Soroush Rais-Bahrami, MD**[1,5], **Kristin K. Porter, MD, PhD**[1], **Gagandeep Choudhary, MD**[1], **Constantine Burgan, MD**[1], **Pradeep Bhambhvani, MD**[1], **Jeffrey W. Nix, MD**[2,5], **Desiree E. Morgan, MD**[1,2], **Yufeng Li, PhD**[1,2,6], **John V. Thomas, MD**[1], **Jonathan McConathy, MD, PhD**[1,2]

[1]Department of Radiology, University of Alabama at Birmingham, 619 19th St S, JT N325, Birmingham, AL 35249.

[2]O'Neal Comprehensive Cancer Center at UAB, University of Alabama at Birmingham, Birmingham, AL.

[3]Department of Radiation Oncology, University of Alabama at Birmingham, Birmingham, AL.

[4]Institute for Cancer Outcomes and Survivorship, University of Alabama at Birmingham, Birmingham, AL.

[5]Department of Urology, University of Alabama at Birmingham, Birmingham, AL.

[6]Division of Preventive Medicine, University of Alabama at Birmingham, Birmingham, AL.

Abstract

BACKGROUND.—Despite advances in prostate cancer treatment, rates of biochemical recurrence remain high, relating to lack of detection of small-volume metastatic disease using conventional imaging for initial staging.

OBJECTIVE.—The purpose of this study was to assess the potential use of ^{18}F-fluciclovine PET/MRI for initial staging of high-risk prostate cancer and evaluating response to androgen deprivation therapy (ADT).

METHODS.—This prospective clinical trial enrolled 14 men with newly diagnosed high-risk prostate cancer and negative or equivocal conventional staging imaging for metastatic disease between January 2018 and February 2019. All patients underwent pretreatment ^{18}F-fluciclovine PET/MRI including multiparametric prostate MRI; 12 underwent ^{18}F-fluciclovine PET/MRI

after surgery or between ADT and radiotherapy. Confidence in identification of the primary intraprostatic lesion and nodal metastases was independently rated on a 0–3 Likert scale by three readers with nuclear medicine experience for ^{18}F-fluciclovine PET/MRI and three readers with abdominal imaging experience for MRI alone. Findings scored as 2 or 3 by at least two readers of a given modality were considered positive. A single reader measured SUV_{mean}, SUV_{max}, and volume of the MRI-defined intraprostatic lesion and SUV_{max} of suspicious lymph nodes on PET before and after initiation of ADT. Changes in SUV were analyzed using nonparametric Wilcoxon signed-rank tests.

RESULTS.—The biopsy-proven lesion in the prostate gland was accurately identified in all 14 patients on both MRI and ^{18}F-fluciclovine PET/MRI. Suspected nodal metastases were detected in three patients on MRI and seven patients on ^{18}F-fluciclovine PET/MRI. After ADT, all patients showed decreased activity within the intraprostatic lesion and/or all suspicious lymph nodes. The primary lesion SUV_{mean} was 4.5 ± 1.1 (range, 2.7–6.5) before treatment and 2.4 ± 1.1 (range, 0.0–3.6) after initiation of ADT ($p = .008$). For suspicious lymph nodes, the pretreatment SUV_{max} was 5.5 ± 3.7 (range, 2.8–12.7) and the posttreatment SUV_{max} was 2.8 ± 1.4 (range, 1.4–5.5) ($p = .03$).

CONCLUSION.—[18]F-labeled fluciclovine PET/MRI shows potential utility in initial staging of high-risk prostate cancer and in evaluating response to ADT.

CLINICAL IMPACT.—Given the FDA approval and widespread availability of ^{18}F-fluciclovine, the findings could have an impact in the immediate future in guiding initial management of patients with prostate cancer.

TRIAL REGISTRATION.—ClinicalTrials.gov NCT03264456

Keywords

androgen deprivation therapy; fluciclovine; PET/MRI; prostate cancer

Prostate cancer is a common malignancy with an estimated 174,650 new cases and 31,620 deaths in 2019 [1]. Approximately 80% of cancers detected are localized to the prostate gland, but a minority of patients have metastatic disease at time of diagnosis. Disease risk is stratified using the Gleason score, serum PSA level, and clinical stage. These provide estimated risks of extraprostatic disease according to established nomograms and Partin tables [2, 3]. Radiologic staging is performed with CT or MRI and skeletal scintigraphy [4]. In patients who undergo definitive treatment, up to 30% experience biochemical recurrence [5, 6]. These recurrences are thought to be a result of lack of detection of small-volume metastatic disease by conventional imaging [7]. Improved imaging is needed to better guide treatment decisions and decrease the rate of biochemical recurrence [8]. Controversy also persists regarding the utility of nodal dissection and/or elective nodal radiation in prostate cancer; improved staging imaging could help to guide these treatments, potentially in a targeted fashion [9-11].

Although prostate MRI is valuable for the detection of primary intraprostatic lesions, its sensitivity and specificity for the detection of nodal metastases are limited by size and nodal morphology [12, 13]. It is well known that normal-appearing lymph nodes on CT

and MRI can harbor metastatic disease [14-18]. In 2016, ^{18}F-fluciclovine (^{18}F-1-amino-3-fluorocyclobutane-1-carboxylic acid) was approved for PET in men with suspected prostate cancer recurrence according to elevated serum PSA levels after prior treatment. ^{18}F-labeled fluciclovine PET/CT has been shown to be effective for detecting nodal metastases and distant metastases in recurrent prostate cancer, and ^{18}F-fluciclovine PET is now incorporated into the National Comprehensive Cancer Network guidelines in the recurrence setting [4, 19-21]. In addition, studies show that ^{18}F-fluciclovine PET/CT results in changes to radiotherapy planning for a majority of patients, and that ^{18}F-fluciclovine PET can be used to develop personalized radiotherapy plans for patients [22-24]. In comparison, limited but promising data support the utility of ^{18}F-fluciclovine PET/CT and PET/MRI for initial staging in prostate cancer [25-30].

An in vitro study of human prostate cancer cells showed significant effects of both 5α-dihydrotestosterone and bicalutamide in the castrate-sensitive setting [31]. However, to the authors' knowledge, no study has evaluated the effect of androgen deprivation therapy (ADT) on ^{18}F-fluciclovine uptake or the use of ^{18}F-fluciclovine PET in evaluating response to ADT in vivo. We hypothesized that ^{18}F-fluciclovine PET/MRI would detect more metastatic disease in pelvic lymph nodes compared with MRI alone and that ^{18}F-fluciclovine PET would show decreased activity within suspicious lesions after initiation of ADT. To determine if future larger studies are justified, this prospective pilot study was conducted to assess the potential use of ^{18}F-fluciclovine PET/MRI for initial staging of high-risk prostate cancer and evaluation of response to ADT.

Methods

Enrollment and Study Design

After local IRB approval, the study was registered as a single-arm prospective pilot clinical trial through ClinicalTrials.gov (NCT03264456); the full protocol is accessible through the trial webpage. The trial took place between January 2018 and February 2019. Written informed consent was obtained from all patients at time of enrollment. A study flowchart is depicted in Figure 1. Inclusion criteria were adult (> 18 years) men who had biopsy-proven treatment-naïve prostate cancer and met National Comprehensive Cancer Network criteria for high-risk or very high-risk prostate cancer (Gleason score 8 and/or a serum PSA 20 ng/mL). All patients underwent a standard-of-care transrectal ultrasound-guided prostate biopsy at time of diagnosis, which included standard 12-core template biopsies with or without the addition of MRI-targeted biopsy. All patients enrolled in the study had negative or equivocal standard-of-care staging imaging for both locoregional and distant metastatic disease, including CT of the abdomen and pelvis or MRI of the pelvis, and whole-body planar ^{99m}Tc-methylene diphosphonate skeletal scintigraphy. Negative standard-of-care imaging was defined as no evidence of metastatic disease by RECIST 1.1 criteria and Prostate Cancer Working Group criteria. Equivocal imaging was defined as lymph nodes approaching the RECIST 1.1 size criteria for enlargement and/or abnormal suspicious morphology in a nonenlarged lymph node. Exclusion criteria included inability to tolerate the PET/MRI scan, history of a hematologic/lymphatic disorder (including lymphoma, leukemia, and Castleman's disease), definite distant metastatic disease on conventional

staging imaging, or allergy to glucagon or gadolinium-based MRI contrast agents. Patients with known distant metastatic disease on conventional imaging were not included given the smaller potential impact of ^{18}F-fluciclovine PET/MRI on their staging. No restriction was placed on the time interval between diagnosis and initial staging PET/MRI, but all patients underwent ^{18}F-fluciclovine PET/MRI before initiation of any therapy.

Acquisition of ^{18}F-Fluciclovine PET/MRI

All patients underwent a ^{18}F-fluciclovine PET/MRI study on a 3-T Signa PET/MRI scanner (GE Healthcare) and received a standard IV dose of 370 MBq of ^{18}F-fluciclovine. Before injection of the radiotracer, all patients underwent standard preparation for ^{18}F-fluciclovine PET and prostate MRI, including avoidance of strenuous exercise for 24 hours before scan, nothing to eat or drink 4 hours before scan, and voiding before scan. PET images were obtained immediately after radiotracer injection for an 8-minute bed position in the pelvis, followed by 5-minute PET acquisitions at six total bed positions. The initial pelvic bed position was acquired immediately to obtain dynamic PET data for the initial 3 minutes, followed by a standard 5-minute PET bed acquisition. The PET reconstruction voxel size was $3.12 \times 3.12 \times 2.78$ mm. The whole-body MRI protocol included axial SSFSE T2-weighted images, axial fat-saturated T1-weighted images, and sagittal nonfat-saturated T1-weighted images. MRI-based attenuation correction was performed with the Dixon method. Additionally, a dedicated regional multiparametric MRI of the prostate (including small FOV T2-weighted images, high b value DWI up to 2000 s/mm^2 [0, 500, 1200, 2000], and dynamic contrast-enhanced images) was obtained as part of the PET/MRI examination.

Treatment decisions were made on the basis of standard-of-care imaging and clinical patient characteristics. If the ^{18}F-fluciclovine PET/MRI findings would potentially alter staging (e.g., show distant metastatic disease), the treating clinician was notified and a biopsy was performed when it was deemed feasible and clinically appropriate. For those patients who proceeded to surgery, a radical prostatectomy and templated extended pelvic lymph node dissection (including the internal iliac, obturator, common iliac, and presacral lymph nodes) was performed as standard of care for high-risk prostate cancer. Patients underwent a repeat ^{18}F-fluciclovine PET/MRI scan using the same protocol described for the pretreatment PET/MRI scan either after radical prostatectomy or 6 to 8 weeks after neoadjuvant ADT but before radiation therapy.

Analysis of ^{18}F-Fluciclovine PET/MRI and Prostate MRI

Whole-body PET/MRI was analyzed on MIM Encore (MIM Software) by three physicians with subspecialty expertise in nuclear medicine (P.B., J.M., and G.C., with 15, 10, and 2 years of experience, respectively). Two of the PET/MRI readers (J.M. and G.C.) are dual–board certified in radiology and nuclear medicine. Prostate MRI was independently interpreted on a dedicated PACS by three radiologists with subspecialty expertise in abdominal imaging (D.E.M., K.K.P., and C.B. with 17, 5, and 4 years of experience, respectively). All readers were unaware of the clinical history and detailed patient information but aware of the diagnosis of prostate cancer. PET/MRI was interpreted and analyzed using the established criteria for interpretation of ^{18}F-fluciclovine PET in the setting of biochemically recurrent prostate cancer [32]. Confidence in identification of the

lesion within the prostate gland, seminal vesicle invasion, extraprostatic extension, and nodal/skeletal metastatic disease was rated on a Likert scale ranging from 0 to 3. A rating of 0 indicated no definite evidence of malignancy, whereas a rating of 1 indicated equivocal for malignancy, 2 indicated suspicious for malignancy, and 3 indicated highly suspicious for or definite malignancy. Likert scale ratings of 0 and 1 were considered a negative imaging finding and Likert scale ratings of 2 and 3 were considered positive imaging findings. PI-RADS criteria were used for the interpretation of the prostate MRI, but a formal PI-RADS score was not recorded. This was primarily because PI-RADS plays a larger role in lesion detection than in locoregional staging. Interreader agreement in imaging findings was measured using intraclass coefficients. The MRI-defined intraprostatic lesion SUV_{mean}, SUV_{max}, volume, and total lesion activity (SUV_{mean} multiplied by lesion volume) were measured by a single reader (S.G., with dual board certification with 3 years of experience) on the summed 5- to 10-minute reconstructed PET images both before and after the initiation of ADT in the patient cohort undergoing radiation therapy. MRI-defined lesions were segmented on the T2-weighted images, and PET ROIs were manually drawn on the MRI-defined lesions. The SUV_{max} of patients with suspicious lymph nodes identified on pretreatment PET/MRI was also evaluated before and after ADT. In the presence of small lymph nodes that were qualitatively positive but challenging to quantitate because of small size, the lymph node with the highest SUV_{max} was selected to best differentiate measurements from background activity.

Statistical Analysis

The primary endpoint of the study was to evaluate the frequency of detection of suspected metastatic disease with ^{18}F-fluciclovine PET/MRI compared with conventional imaging with MRI for patients with newly diagnosed high-risk prostate cancer. Findings rated as Likert scale 2 or 3 by two or more readers were considered positive, and findings rated as Likert scale 0 or 1 by two or more readers were considered negative. Interreader agreement was calculated on the basis of classification of the nodal station or finding as either positive or negative. The secondary endpoint was to evaluate changes in SUV in prostatic lesions and suspicious lymph nodes in patients undergoing neoadjuvant ADT. Given that this study was a pilot study, no formal power calculations were used in the generation of sample size. Changes in SUV were analyzed using the nonparametric Wilcoxon signed rank test. Any p values < .05 were considered statistically significant.

Results

Demographics and Patient Characteristics

A total of 14 patients were enrolled in the study and underwent ^{18}F-fluciclovine PET/MRI before treatment. Patient demographics are summarized in Table 1. Recruitment was completed when the prespecified number of patients per the study's funding was reached. Primary tumor Gleason scores were 3 + 4 ($n = 2$), 4 + 3 ($n = 3$), 4 + 4 ($n = 4$), and 4 + 5 or 5 + 4 ($n = 5$). Multifocal prostate cancer was present in biopsy specimens in five patients at the time of initial diagnosis. The mean pretreatment serum PSA value was 33.0 ± 28.7 ng/mL (range, 2.8–100). According to standard-of-care Partin tables, the study participants had a mean predicted risk of lymph node metastases of 21% (range, 6–48%).

Initial Staging With ^{18}F-Fluciclovine PET/MRI

Results for initial staging with ^{18}F-fluciclovine PET/MRI are summarized in Table 2. Full results are available in Supplemental Tables S1 and S2 in the online supplement to this article at doi.org/10.2214/AJR.20.24509. The biopsy-proven lesion in the prostate gland was accurately identified in all 14 patients on both pretreatment MRI and PET/MRI, and the activity noted on PET/MRI correlated with both the MRI-defined intraprostatic lesions and biopsy-proven prostate cancer (Fig. 2). All patients in the study had a single intraprostatic lesion, although five patients had a diffuse tumor that occupied most of the prostate gland. Suspected seminal vesicle invasion was detected on PET/MRI in a total of four patients, two of the seminal vesicle invasions were detected only on the PET/MRI and not on the regional prostate MRI performed as part of the PET/MRI protocol. Suspected pelvic regional nodal metastases were detected in three patients on MRI alone and in seven patients on PET/MRI (Fig. 3). Of the three patients with suspected pelvic regional nodal metastases on MRI, ^{18}F-fluciclovine PET/MRI was concordant for lymph node metastases and showed additional suspected lymph node metastases not detected on MRI alone. Of the patients who proceeded to surgery, no lymph node metastases were detected on ^{18}F-fluciclovine PET/MRI nor on surgical pathology. Two patients were found to have nonregional suspected nodal metastases on PET/MRI that were not detected on MRI. No skeletal metastases were detected in any enrolled patients. In patients who underwent surgical resection and posttreatment PET/MRI, no residual prostatic tissue or abnormal PET activity in the prostate bed was identified. No patient experienced adverse effects from the ^{18}F-fluciclovine PET/MRI during the trial.

Interreader Agreement and Pathologic Confirmation of Staging Findings

Interreader agreement for assessment of nodal metastatic disease was high on both MRI and PET/MRI, with intraclass coefficients greater than 0.90 for nine of 11 pelvic nodal stations analyzed for MRI both before and after treatment, and greater than 0.90 for eight of 11 pelvic nodal stations analyzed for PET/MRI before and after treatment (Table 3). A total of two nodal biopsies were performed as part of this trial. One biopsy of an ischiorectal fossa lymph node rated as a Likert scale 3 (highly suspicious for or definite malignancy) was found to represent metastatic prostate carcinoma. A second biopsy of a retroperitoneal lymph node rated as a Likert scale 2 (suspicious for malignancy) was found to represent a benign lymph node. One patient with suspected seminal vesicle invasion on PET/MRI but not the MRI alone underwent surgery and was histologically confirmed to have seminal vesicle invasion at radical prostatectomy.

Restaging Using ^{18}F-Fluciclovine PET/MRI After Androgen Deprivation Therapy

Ten of the 14 (71.4%) patients underwent ADT before radiation therapy. Primary tumor Gleason scores were 3 + 4 ($n = 2$), 4 + 3 ($n = 2$), 4 + 4 ($n = 3$), and 4 + 5 or 5 + 4 ($n = 3$). The mean pretreatment serum PSA value of this subgroup was 33.0 ± 22.9 ng/mL (range, 2.8–76.5). The mean serum PSA value 6 weeks after initiation of ADT was 2.1 ng/mL (range, 0.3–5.7) (Table 1). Results for the cohort undergoing ADT before radiation therapy are summarized in Table 4. Full results are available in Supplemental Tables S3 and S4 in the online supplement to this article at doi.org/10.2214/AJR.20.24509. The primary intraprostatic lesion was accurately identified in all 10 patients, seven of whom showed

suspicious lymph nodes on the pretreatment PET/MRI. After ADT, all 10 patients showed a decrease in tracer activity either within the primary intraprostatic lesion, all suspicious lymph nodes detected on the pretreatment ^{18}F-fluciclovine PET/MRI, or both (Fig. 4). Suspected metastatic lesions on the PET scan before ADT were not visible in three of seven patients after the initiation of ADT. The primary lesion SUV_{mean} was 4.5 ± 1.1 (range, 2.7–6.5) before treatment and 2.4 ± 1.1 (range, 0.0–3.6) after initiation of ADT ($p = .008$). The primary lesion SUV_{max} was 7.1 ± 1.7 (range, 3.9–8.6) before treatment and 3.5 ± 2.0 (range, 0.0–7.6) after initiation of ADT ($p = .008$). The pretreatment PET/MRI-segmented lesion volume (mL) was 8.7 ± 10.5 (range, 0.5–27.4) and the posttreatment volume was 2.4 ± 4.0 (range, 0–12.7) ($p = .004$). The pretreatment total lesion activity was 39.8 ± 49.5 (range, 1.8–132.2) and posttreatment total lesion activity was 7.1 ± 12.3 (range, 0.0–39.0) ($p = .004$). In patients with suspicious lymph nodes detected on pretreatment PET/MRI, the pretreatment SUV_{max} was 5.5 ± 3.7 (range, 2.8–12.7) and posttreatment SUV_{max} was 2.8 ± 1.4 (range, 1.4–5.5) ($p = .03$). A plot of changes in PSA level and prostatic lesion SUV_{max} is depicted in Figure 5.

Discussion

Our prospective pilot study shows the potential of ^{18}F-fluciclovine PET/MRI to improve the initial staging of patients with high-risk prostate cancer. There was high correlation between the MRI-defined lesion and ^{18}F-fluciclovine PET/MRI-defined activity, which concurs with prior published data [28]. Further, in two patients, ^{18}F-fluciclovine PET/MRI showed seminal vesicle invasion that was not identified on MRI, thereby improving T categorization; this detection of seminal vesicle invasion could direct image-guided seminal vesicle biopsy and is particularly important in patients not undergoing radical prostatectomy [33]. The seminal vesicle invasion could be missed during initial workup if only performing PET/MRI after the administration of ADT. Moreover, in half of the patients in our sample, ^{18}F-fluciclovine PET/MRI detected suspected metastatic lymph nodes that were not enlarged according to RECIST 1.1 criteria, similar to the reported performance of ^{18}F-fluciclovine PET in the setting of initial staging [26]. In comparison with the biochemical recurrence setting, little data exist regarding this specific benefit of ^{18}F-fluciclovine PET relative to conventional imaging during initial staging [23]. Detection of these lymph nodes during initial staging may have important consequences for surgery or radiotherapy planning. Thus, our study results support the potential utility of ^{18}F-fluciclovine PET in initial staging when compared with conventional imaging with superior detection of extraprostatic disease. Additionally, although not the focus of this study, ^{18}F-fluciclovine PET/MRI offers far superior intraprostatic lesion characterization and local staging of the prostate when compared with PET/CT because of the superiority of multiparametric prostate MRI performed during the examination and increasing characterization of fluciclovine-PET activity within the gland.

Several prior studies have validated ^{18}F-fluciclovine uptake on initial staging PET as a marker of metastatic disease with subsequent pathologic confirmation [26, 28, 34]. In a study of ^{18}F-fluciclovine PET/MRI for detection and characterization of high-risk prostate cancer in patients undergoing radical prostatectomy, Elschot et al. [28] found that ^{18}F-fluciclovine PET/MRI outperformed both MRI and PET alone in distinguishing malignant

from benign tissue and high-grade tumors from other tissues. Selnaes et al. [26] found that in high-risk patients undergoing radical prostatectomy, fluciclovine PET/MRI activity in lymph nodes was highly specific for the presence of metastatic disease at resection. A recent study by Alemozaffar et al. [34] of 68 patients with high-risk prostate cancer undergoing radical prostatectomy established a per-patient specificity of 84.8% in the detection of metastatic disease in lymph nodes and showed significantly higher sensitivity compared with conventional imaging. Despite the limited pathologic confirmation for staging findings in our study, our findings provide additional evidence in support of the role of ^{18}F-fluciclovine PET/MRI in initial staging of high-risk prostate cancer and illustrates the potential value of PET/MRI via integration of multiparametric prostate MRI to improve characterization of ^{18}F-fluciclovine uptake within the prostate gland, which is a particular advantage over PET/CT.

Fluorine-18-labeled fluciclovine PET/MRI detected suspected pelvic lymph node metastases at a higher rate than expected according to established risk nomograms (50% vs 21%, respectively). If validated in larger studies, new nomograms for primary staging might need to be considered to reflect the increased detection of both locoregional and distant metastatic disease observed in primary staging with ^{18}F-fluciclovine PET. Use of ^{18}F-fluciclovine PET has been shown to aid image-guided targeted biopsies, similar to MRI-targeted biopsies, to correctly stage and risk stratify patients before radical prostatectomy and avoid upstaging of disease on the radical prostatectomy specimen [35, 36]. Additionally, improved detection of suspected nodal metastatic disease outside the pelvis can have important therapeutic consequences and change the patient management [37].

After ADT, patients consistently showed decreases in serum PSA value and decreases in ^{18}F-fluciclovine uptake in primary prostate cancer and nodal metastases. To the authors' knowledge, no published human data exist describing the changes in SUV after ADT. Thus, ^{18}F-fluciclovine PET may be useful in monitoring response to ADT, particularly if there is a failure of expected PSA level decline after therapy. This observation could be beneficial in treatment planning given that patients could potentially be considered for targeted radiotherapy or surgery. Additionally, given that prostate cancer is often multifocal and in varying stages of evolution, a lesion with persistent PET activity after ADT may warrant a focal therapeutic radiation boost to achieve durable response; ^{18}F-fluciclovine PET/MRI could therefore potentially guide brachytherapy if being used adjunctively with ADT. If only the ^{18}F-fluciclovine PET after PET was interpreted to guide therapy, suspected metastatic lesions that were observed on the PET before ADT would have been missed in three of seven patients with positive pretreatment PET. In two patients who underwent ADT, the primary prostatic lesion was no longer visible on the PET after ADT. Therefore, ADT may decrease the detection of metastases with ^{18}F-fluciclovine PET after initiation of neoadjuvant ADT, particularly in the absence of a pretreatment PET.

Prostate-specific membrane antigen (PSMA) PET radiotracers are a class of radiopharmaceuticals that target the PSMA transmembrane protein, which is overexpressed in prostate cancer cells. Early data suggest that PSMA tracers have superior diagnostic performance compared with ^{18}F-fluciclovine in both initial staging and biochemical recurrence settings [38, 39]. In a head-to-head prospective study performed by Calais et al.

[38], PSMA radiotracers outperformed ^{18}F-fluciclovine for the detection of biochemically recurrent prostate cancer in all anatomic regions except for the prostate bed. A recent meta-analysis of the performance of all PSMA radiotracers and ^{18}F-fluciclovine in the setting of biochemical recurrence showed superior performance of PSMA radiotracers for patients with PSA values of 1.0–1.9 ng/mL [40]. Additionally, the diagnostic accuracy of ^{68}Ga-PSMA-11 PET/MRI compared with multiparametric MRI for the detection of prostate cancer showed superior detection of prostate cancer within the prostate gland at time of radical prostatectomy [41]. One study observed changes on PSMA PET after neoadjuvant ADT that appear to mirror our findings [42]. However, many PSMA radiotracers use ^{68}Ga, which limits widespread distribution and utilization. Interest is recently increasing in the development of ^{18}F-labeled PSMA compounds. However, these tracers are still in development, and how their performance compares to ^{68}Ga-labeled PSMA tracers is unclear [43]. At this time, no PSMA PET radiotracer is approved by the FDA. Although FDA approval of one or more PSMA PET ligands is expected in the near future, their use is currently limited to the research setting. To our knowledge, no current published data directly compare PSMA ligands and ^{18}F-fluciclovine in assessing response to ADT.

Our study is limited by small sample size and the lack of pathologic confirmation of ^{18}F-fluciclovine PET/MRI findings outside of the biopsy-proven prostate cancer. However, prior studies have shown high specificity between ^{18}F-fluciclovine PET/MRI detection of nodal metastases and pathologic confirmation of malignancy in patients who underwent radical prostatectomy [26]. Additionally, multiple lymph nodes that were not biopsied or surgically removed showed decreased activity and/or resolution on ^{18}F-fluciclovine PET/MRI after ADT. Thus, it is inferred that the findings on the ^{18}F-fluciclovine PET/MRI examinations reflect true-positive sites of disease. In the two patients who underwent biopsy in our study, one of the two samples was a true metastasis and the other represented a false-positive. The false-positive case did have a lower Likert rating for metastatic disease compared with the true-positive, although it is difficult to draw a meaningful conclusion given the small number of lymph node biopsies performed as part of this study. On the PET/MRI scan after therapy, the qualitative appearance of the false-positive lymph node did not change and no size change was observed, consistent with a benign lymph node. Additionally, given the single reader for the quantitative measurements, future studies with larger patient cohorts will be required to assess the reproducibility of quantitative data.

This prospective pilot study provides an important preliminary step in establishing the utility of ^{18}F-fluciclovine PET/MRI in the initial staging of men with high-risk prostate cancer and builds on previously published data. Larger multicenter trials with pathologic confirmation and patient outcomes as the reference standard are needed to validate the findings. Our study is also the first to our knowledge to prospectively examine use of ^{18}F-fluciclovine PET in evaluating response to ADT in vivo. Knowledge of the impact of ADT on the findings on ^{18}F-fluciclovine PET is important, particularly in staging of castrate-sensitive disease. Thus, ^{18}F-fluciclovine PET/MRI allows a comprehensive initial staging of high-risk prostate cancer in a single session, and the components of the examination provide complementary information. Given the FDA approval of ^{18}F-fluciclovine, this study could have widespread impact in the immediate future in guiding initial management of patients with prostate cancer.

Supplementary Material

Refer to Web version on PubMed Central for supplementary material.

Acknowledgments

References

1. Howlader N, Noone A, Krapcho M, et al. (eds). SEER cancer statistics review, 1975–2013. National Cancer Institute, 2016

2. Eifler JB, Feng Z, Lin BM, et al. An updated prostate cancer staging nomogram (Partin tables) based on cases from 2006 to 2011. BJU Int 2013; 111:22–29 [PubMed: 22834909]

3. Kattan MW, Eastham JA, Stapleton AM, Wheeler TM, Scardino PT. A preoperative nomogram for disease recurrence following radical prostatectomy for prostate cancer. J Natl Cancer Inst 1998; 90:766–771 [PubMed: 9605647]

4. Mohler JL, Antonarakis ES, Armstrong AJ, et al. Prostate cancer, version 2.2019, NCCN clinical practice guidelines in oncology. J Natl Compr Canc Netw 2019; 17:479–505 [PubMed: 31085757]

5. Rosenbaum E, Partin A, Eisenberger MA. Biochemical relapse after primary treatment for prostate cancer: studies on natural history and therapeutic considerations. J Natl Compr Canc Netw 2004; 2:249–256 [PubMed: 19795608]

6. Han M, Partin AW, Zahurak M, Piantadosi S, Epstein JI, Walsh PC. Biochemical (prostate specific antigen) recurrence probability following radical prostatectomy for clinically localized prostate cancer. J Urol 2003; 169:517–523 [PubMed: 12544300]

7. Moghanaki D, Turkbey B, Vapiwala N, et al. Advances in prostate cancer magnetic resonance imaging and positron emission tomography-computed tomography for staging and radiotherapy treatment planning. Semin Radiat Oncol 2017; 27:21–33 [PubMed: 27986208]

8. Bagheri MH, Ahlman MA, Lindenberg L, et al. Advances in medical imaging for the diagnosis and management of common genitourinary cancers. Urol Oncol 2017; 35:473–491 [PubMed: 28506596]

9. Pommier P, Chabaud S, Lagrange JL, et al. Is there a role for pelvic irradiation in localized prostate adenocarcinoma? Update of the long-term survival results of the GETUG-01 randomized study. Int J Radiat Oncol Biol Phys 2016; 96:759–769 [PubMed: 27788949]

10. Roach M, Moughan J, Lawton CAF, et al. Sequence of hormonal therapy and radiotherapy field size in unfavourable, localised prostate cancer (NRG/RTOG 9413): long-term results of a randomised, phase 3 trial. Lancet Oncol 2018; 19:1504–1515 [PubMed: 30316827]

11. Fossati N, Willemse PM, Van den Broeck T, et al. The benefits and harms of different extents of lymph node dissection during radical prostatectomy for prostate cancer: a systematic review. Eur Urol 2017; 72:84–109 [PubMed: 28126351]

12. Truong M, Wang B, Gordetsky JB, et al. Multi-institutional nomogram predicting benign prostate pathology on magnetic resonance/ultrasound fusion biopsy in men with a prior negative 12-core systematic biopsy. Cancer 2018; 124:278–285 [PubMed: 28976544]

13. Zarzour JG, Galgano S, McConathy J, Thomas JV, Rais-Bahrami S. Lymph node imaging in initial staging of prostate cancer: an overview and update. World J Radiol 2017; 9:389–399 [PubMed: 29104741]

14. Sider L, Horejs D. Frequency of extrathoracic metastases from bronchogenic carcinoma in patients with normal-sized hilar and mediastinal lymph nodes on CT. AJR 1988; 151:893–895 [PubMed: 2845761]

15. Forsberg L, Dale L, Høiem L, et al. Computed tomography in early stages of testicular carcinoma. Size of normal retroperitoneal lymph nodes and lymph nodes in patients with metastases in stage

II A. A SWENOTECA study: Swedish-Norwegian Testicular Cancer Project. Acta Radiol Diagn (Stockh) 1986; 27:569–574 [PubMed: 3026141]

16. Gritters LS, Francis IR, Zasadny KR, Wahl RL. Initial assessment of positron emission tomography using 2-fluorine-18-fluoro-2-deoxy-D-glucose in the imaging of malignant melanoma. J Nucl Med 1993; 34:1420–1427 [PubMed: 8355058]

17. Heesakkers RA, Hovels AM, Jager GJ, et al. MRI with a lymph-node-specific contrast agent as an alternative to CT scan and lymph-node dissection in patients with prostate cancer: a prospective multicohort study. Lancet Oncol 2008; 9:850–856 [PubMed: 18708295]

18. Thoeny HC, Triantafyllou M, Birkhaeuser FD, et al. Combined ultrasmall superparamagnetic particles of iron oxide-enhanced and diffusion-weighted magnetic resonance imaging reliably detect pelvic lymph node metastases in normal-sized nodes of bladder and prostate cancer patients. Eur Urol 2009; 55:761–769 [PubMed: 19144456]

19. Schuster DM, Savir-Baruch B, Nieh PT, et al. Detection of recurrent prostate carcinoma with anti-1-amino-3-^{18}F-fluorocyclobutane-1-carboxylic acid PET/CT and ^{111}In-capromab pendetide SPECT/CT. Radiology 2011; 259:852–861 [PubMed: 21493787]

20. Bach-Gansmo T, Nanni C, Nieh PT, et al. Multisite experience of the safety, detection rate and diagnostic performance of fluciclovine (^{18}F) positron emission tomography/computerized tomography imaging in the staging of biochemically recurrent prostate cancer. J Urol 2017; 197:676–683 [PubMed: 27746282]

21. Andriole GL, Kostakoglu L, Chau A, et al. ; LOCATE Study Group. The impact of positron emission tomography with ^{18}F-fluciclovine on the treatment of biochemical recurrence of prostate cancer: results from the LOCATE trial. J Urol 2019; 201:322–331 [PubMed: 30179618]

22. McDonald AM, Galgano SJ, McConathy JE, et al. Feasibility of dose escalating [^{18}F]fluciclovine positron emission tomography positive pelvic lymph nodes during moderately hypofractionated radiation therapy for high-risk prostate cancer. Adv Radiat Oncol 2019; 4:649–658 [PubMed: 31673658]

23. Akin-Akintayo OO, Jani AB, Odewole O, et al. Change in salvage radiotherapy management based on guidance with FACBC (fluciclovine) PET/CT in postprostatectomy recurrent prostate cancer. Clin Nucl Med 2017; 42:e22–e28 [PubMed: 27749412]

24. Jani AB, Schreibmann E, Rossi PJ, et al. Impact of ^{18}F-fluciclovine PET on target volume definition for postprostatectomy salvage radiotherapy: initial findings from a randomized trial. J Nucl Med 2017; 58:412–418 [PubMed: 27609792]

25. Suzuki H, Jinnouchi S, Kaji Y, et al. Diagnostic performance of ^{18}F-fluciclovine PET/CT for regional lymph node metastases in patients with primary prostate cancer: a multicenter phase II clinical trial. Jpn J Clin Oncol 2019; 49:803–811 [PubMed: 31095314]

26. Selnaes KM, Krüger-Stokke B, Elschot M, et al. ^{18}F-fluciclovine PET/MRI for preoperative lymph node staging in high-risk prostate cancer patients. Eur Radiol 2018; 28:3151–3159 [PubMed: 29294158]

27. Jambor I, Kuisma A, Kähkönen E, et al. Prospective evaluation of ^{18}F-FACBC PET/CT and PET/MRI versus multiparametric MRI in intermediate- to high-risk prostate cancer patients (FLUCIPRO trial). Eur J Nucl Med Mol Imaging 2018; 45:355–364 [PubMed: 29147764]

28. Elschot M, Selnaes KM, Sandsmark E, et al. Combined ^{18}F-fluciclovine PET/MRI shows potential for detection and characterization of high-risk prostate cancer. J Nucl Med 2018; 59:762–768 [PubMed: 28986510]

29. Elschot M, Selnaes KM, Sandsmark E, et al. A PET/MRI study towards finding the optimal [^{18}F]fluciclovine PET protocol for detection and characterisation of primary prostate cancer. Eur J Nucl Med Mol Imaging 2016; 44:695–703 [PubMed: 27817158]

30. Alemozaffar M, Akintayo AA, Abiodun-Ojo OA, et al. [(18)F]fluciclovine PET/CT for preoperative staging in patients with intermediate to high risk primary prostate cancer. J Urol 2020; 204:734–740 [PubMed: 32347780]

31. Okudaira H, Oka S, Ono M, et al. Accumulation of trans-1-amino-3-[(18)F]fluorocyclobutanecarboxylic acid in prostate cancer due to androgen-induced expression of amino acid transporters. Mol Imaging Biol 2014; 16:756–764 [PubMed: 24943499]

32. Nanni C, Zanoni L, Bach-Gansmo T, et al. [(18)F]Fluciclovine PET/CT: joint EANM and SNMMI procedure guideline for prostate cancer imaging-version 1.0. Eur J Nucl Med Mol Imaging 2020; 47:579–591 [PubMed: 31822959]

33. Gold SA, Shih JH, Rais-Bahrami S, et al. ; Collaborators. When to biopsy the seminal vesicles: a validated multiparametric magnetic resonance imaging and target driven model to detect seminal vesicle invasion in prostate cancer. J Urol 2019; 201:943–949

34. Alemozaffar M, Akintayo AA, Abiodun-Ojo OA, et al. [18F]fluciclovine positron emission tomography/computerized tomography for preoperative staging in patients with intermediate to high risk primary prostate cancer. J Urol 2020; 204:734–740 [PubMed: 32347780]

35. Glaser ZA, Gordetsky JB, Bae S, Nix JW, Porter KK, Rais-Bahrami S. Evaluation of MSKCC preprostatectomy nomogram in men who undergo MRI-targeted prostate biopsy prior to radical prostatectomy. Urol Oncol 2019; 37:970–975 [PubMed: 31495569]

36. Fei B, Abiodun-Ojo OA, Akintayo AA, et al. Feasibility and initial results: fluciclovine positron emission tomography/ultrasound fusion targeted biopsy of recurrent prostate cancer. J Urol 2019; 202:413–421 [PubMed: 30817240]

37. Parker CC, James ND, Brawley CD, et al. ; Systemic Therapy for Advanced or Metastatic Prostate cancer: Evaluation of Drug Efficacy (STAMPEDE) Investigators. Radiotherapy to the primary tumour for newly diagnosed, metastatic prostate cancer (STAMPEDE): a randomised controlled phase 3 trial. Lancet 2018; 392:2353–2366 [PubMed: 30355464]

38. Calais J, Ceci F, Eiber M, et al. 18F-fluciclovine PET-CT and 68Ga-PSMA-11 PET-CT in patients with early biochemical recurrence after prostatectomy: a prospective, single-centre, single-arm, comparative imaging trial. Lancet Oncol 2019; 20:1286–1294 [PubMed: 31375469]

39. Sonni I, Eiber M, Fendler WP, et al. Impact of 68Ga-PSMA-11 PET/CT on staging and management of prostate cancer patients in various clinical settings: a prospective single-center study. J Nucl Med 2020; 61:1153–1160 [PubMed: 31924715]

40. Tan N, Oyoyo U, Bavadian N, et al. PSMA-targeted radiotracers versus 18F fluciclovine for the detection of prostate cancer biochemical recurrence after definitive therapy: a systematic review and meta-analysis. Radiology 2020; 296:44–55 [PubMed: 32396045]

41. Hicks RM, Simko JP, Westphalen AC, et al. Diagnostic accuracy of 68Ga-PSMA-11 PET/MRI compared with multiparametric MRI in the detection of prostate cancer. Radiology 2018; 289:730–737 [PubMed: 30226456]

42. Onal C, Guler OC, Torun N, Reyhan M, Yapar AF. The effect of androgen deprivation therapy on 68Ga-PSMA tracer uptake in non-metastatic prostate cancer patients. Eur J Nucl Med Mol Imaging 2020; 47:632–641 [PubMed: 31732768]

43. Werner RA, Derlin T, Lapa C, et al. 18F-labeled, PSMA-targeted radiotracers: leveraging the advantages of radiofluorination for prostate cancer molecular imaging. Theranostics 2020; 10:1–16 [PubMed: 31903102]

HIGHLIGHTS

Key Finding

- In this prospective pilot study, ^{18}F-fluciclovine PET/MRI identified the biopsy-proven prostatic lesion in all patients, and suspected nodal metastases were detected in three patients on MRI versus seven patients on PET/MRI. After androgen deprivation therapy, all patients showed decreased activity within the intraprostatic lesion and/or all suspicious lymph nodes.

Importance

- ^{18}F-labeled fluciclovine PET/MRI is primarily used in the posttreatment recurrence setting; this study supports its clinical expansion to initial staging of high-risk prostate cancer.
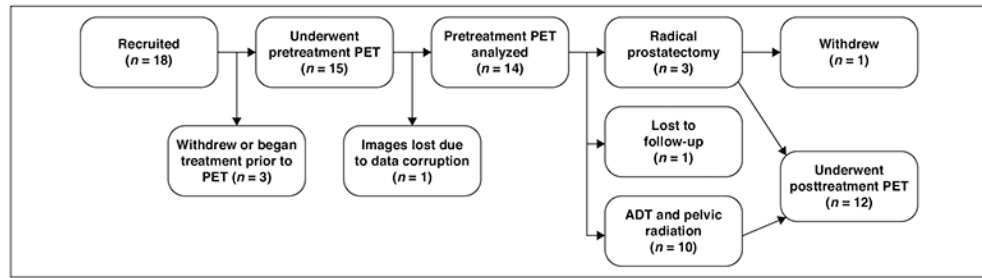
Fig. 1—.

Flowchart of study enrollment and patient follow-up. ADT = androgen deprivation therapy.
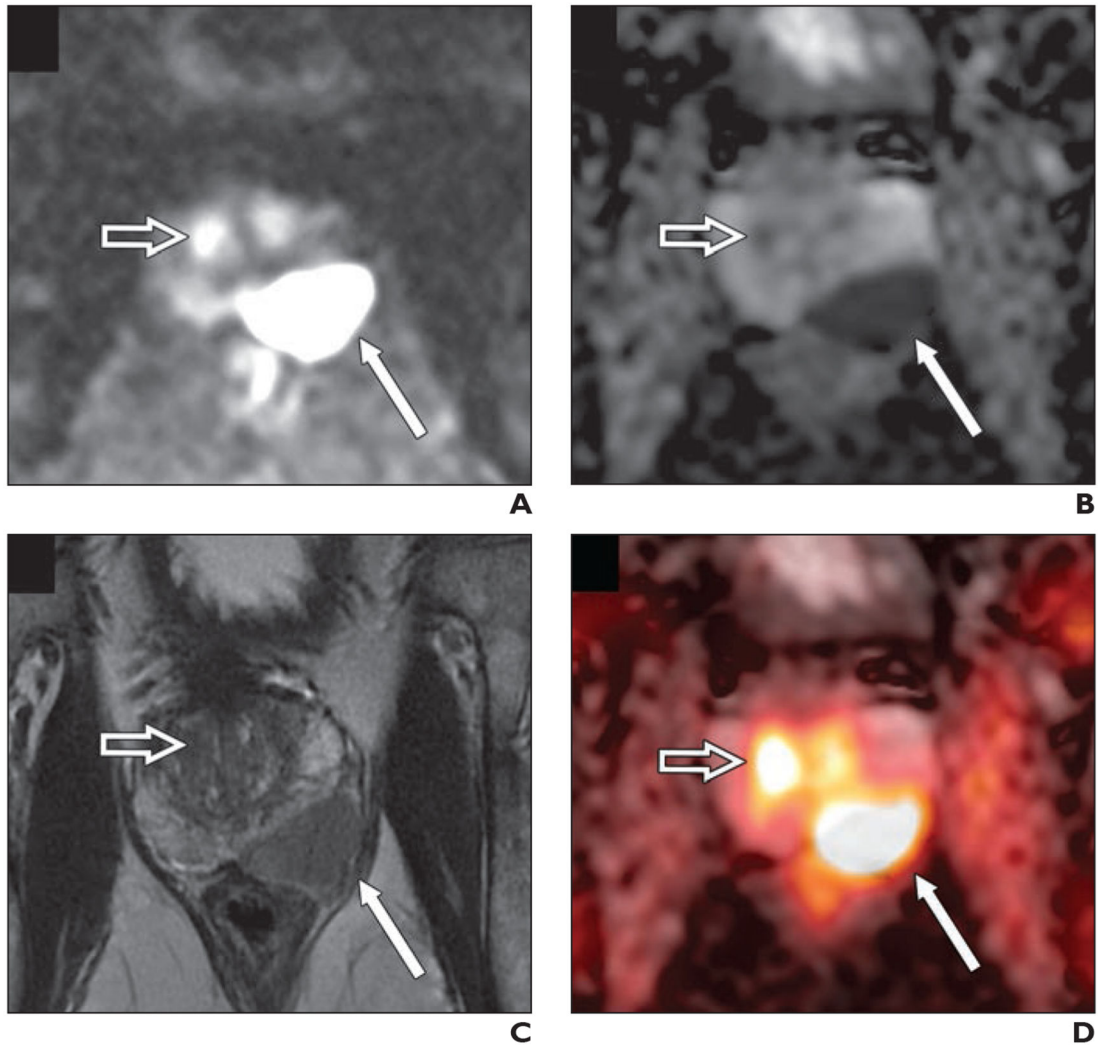
Fig. 2—.

77-year-old man with biopsy-proven Gleason score 4 + 5 prostate cancer in left base and serum PSA level of 8.4 ng/mL with negative conventional staging (no evidence of metastatic disease).

A–C, DWI (b value, 2000 s/mm^2) (**A**), apparent diffusion coefficient map (**B**), and small FOV T2-weighted MRI (**C**) images show large PI-RADS 5 lesion in left base with T2-weighted hypointensity and marked restricted diffusion (*thin arrow*). Open arrow shows uptake in transition zone.

D, Fused ^{18}F-fluciclovine PET/MRI shows high focal activity within lesion (*thin arrow*). Second focus of uptake (*open arrow*) in transition zone with no anatomic lesion on T2-weighted images and mild corresponding restricted diffusion corresponds to benign prostatic hyperplasia nodule.
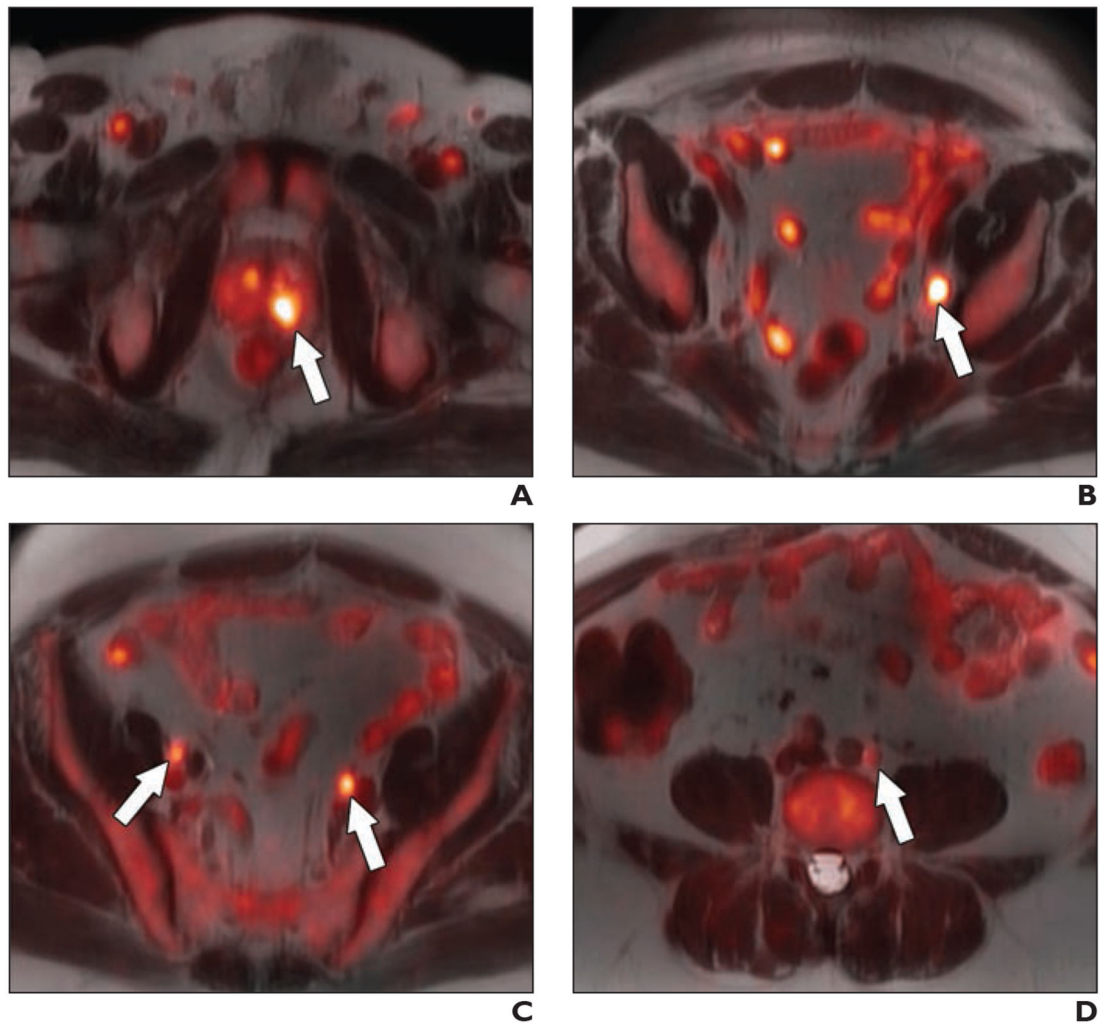
Fig. 3—.

64-year-old man with biopsy-proven Gleason 4 + 5 prostate cancer in left base and serum PSA value of 11.1 ng/mL and equivocal conventional staging with 1.3 cm (borderline enlarged) left internal iliac lymph node.

A–D, Fused ^{18}F-fluciclovine PET/MRI images show high focal uptake within left prostate base (*arrow,* **A**) and left internal iliac lymph node (*arrow,* **B**), and additional subcentimeter bilateral external iliac (*arrows,* **C**) and left common iliac lymph nodes (*arrow,* **D**) suspicious for metastatic disease.
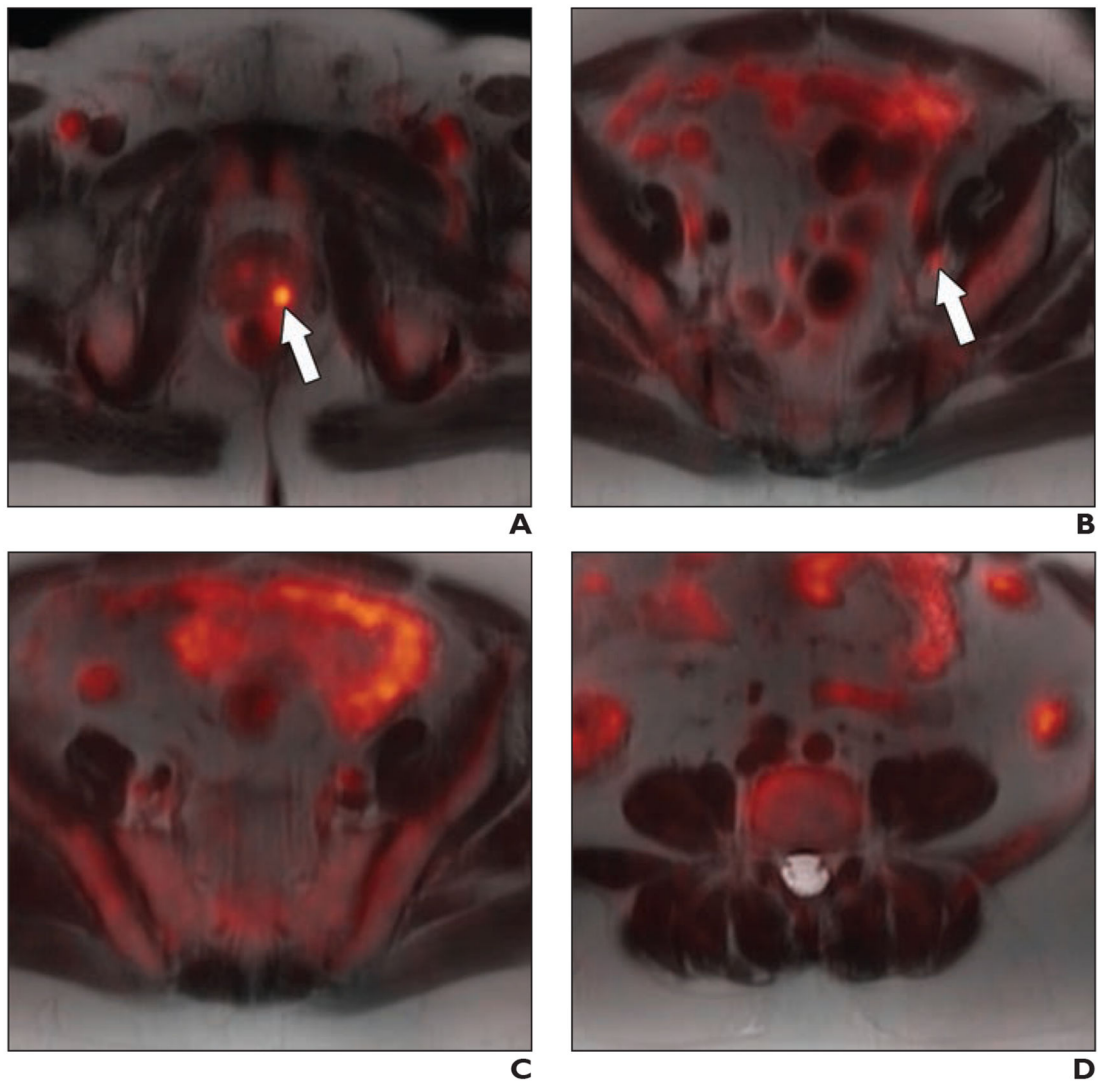
Fig. 4—.
64-year-old man with biopsy-proven Gleason 4 + 5 prostate cancer in left base and serum PSA value of 11.1 ng/mL and equivocal conventional staging with 1.3 cm (borderline enlarged) left internal iliac lymph node (same patient as in Fig. 3) after 6 weeks of androgen deprivation therapy and decrease in serum PSA value from 11.1 to 0.3 ng/mL. **A–D,** Fused ^{18}F-fluciclovine PET/MR images show decreased activity (*arrow,* **A** and **B**) within primary prostate lesion (**A**) and left internal iliac lymph node (**B**), and resolution of activity in additional previously identified suspicious pelvic lymph nodes (**C** and **D**).
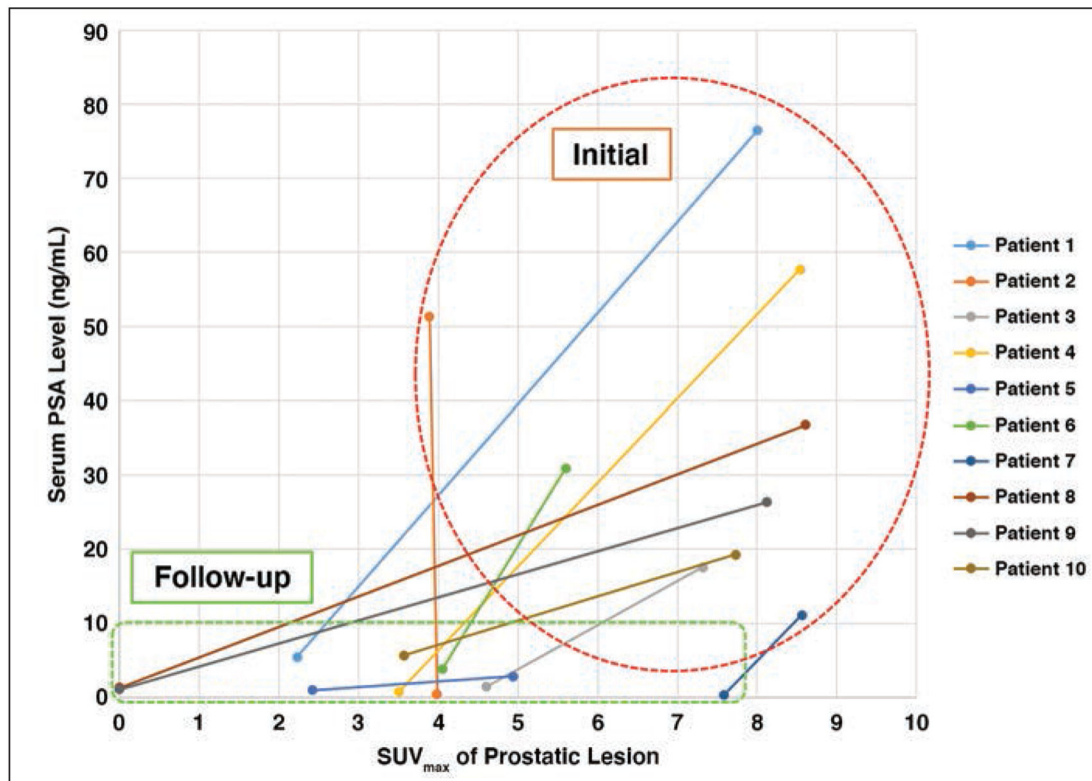
Fig. 5—.

Scatterplot illustrates changes in SUV_{max} of prostatic lesion versus serum PSA level in men before (within *red outline*) and after (within *green outline*) undergoing neoadjuvant androgen deprivation therapy.

TABLE 1:

Patient Demographics

Characteristic	Total Cohort (*n* = 14)	ADT and Radiation Cohort (*n* = 10)
Age (y)		
Mean ± SD	65.6 ± 8.3	64.7 ± 8.8
Range	50–81	50–81
Gleason score (no.)		
3 + 4	2	2
4 + 3	3	2
4 + 4	4	3
4 + 5 or 5 + 4	5	3
PSA level (ng/mL)		
Pretreatment		
Mean ± SD	33.0 ± 28.7	33.0 ± 22.9
Range	2.8–100	2.8–76.5
Posttreatment		
Mean ± SD	NA	2.1 ± 2.0
Range	NA	0.3–5.7
Treatment modality (no.)		
Radical prostatectomy	3	NA
ADT and radiation	10	NA
Lost to follow-up	1	NA

Note—ADT = androgen deprivation therapy, NA = not applicable.

TABLE 2:

Comparison of MRI and ^{18}F-Fluciclovine PET/MRI Results for Initial Staging

Finding	MRI	PET/MRI
Primary lesion	14 (100)	14 (100)
Seminal vesicle invasion	2 (14)	4 (29)
Regional (pelvic) nodal metastases	3 (21)	7 (50)
Nonregional (extrapelvic) metastases	NA	2 (14)

Note—Values are expressed as no. (%) of patients. NA = not applicable.

TABLE 3:

Intraclass Correlation Coefficients of Agreement for Three MRI Readers and Three PET/MRI Readers for Pretreatment and Posttreatment Scans

Lymph Node Station	MRI[a]		PET/MRI	
	Pretreatment	Posttreatment	Pretreatment	Posttreatment
Common iliac				
Right	0.99	1.00	0.99	1.00
Left	1.00	1.00	1.00	1.00
Internal iliac				
Right	0.99	1.00	0.74	0.50
Left	0.50	1.00	1.00	1.00
External iliac				
Right	1.00	0.74	0.51	0.73
Left	0.99	1.00	0.64	0.78
Obturator				
Right	1.00	0.99	1.00	1.00
Left	1.00	1.00	0.99	1.00
Inguinal				
Right	0.99	1.00	1.00	1.00
Left	0.99	1.00	1.00	0.99
Paraaortic	0.99	1.00	1.00	1.00

[a]MRI was performed as part of PET/MRI examination.

TABLE 4:

Changes in SUV in Primary Lesion and Suspicious Lymph Nodes in Patients Undergoing Androgen Deprivation Therapy (ADT)

Characteristic	Before ADT	After ADT	p [a]
Primary lesion			
SUV$_{mean}$			
Mean ± SD	4.5 ± 1.1	2.4 ± 1.1	.008
Median	4.4	2.7	
Minimum	2.7	0	
Maximum	6.5	3.6	
SUV$_{max}$			
Mean ± SD	7.1 ± 1.7	3.5 ± 2.0	.008
Median	7.9	3.6	
Minimum	3.9	0	
Maximum	8.6	7.6	
Volume (mL)			
Mean ± SD	8.7 ± 10.5	2.4 ± 4.0	.004
Median	2.8	1.1	
Minimum	0.5	0	
Maximum	27.4	12.7	
Total lesion activity			
Mean ± SD	39.8 ± 49.5	7.1 ± 12.3	.004
Median	13.2	3.3	
Minimum	1.8	0	
Maximum	132.2	39.0	
Lymph node SUV$_{max}$			
Mean ± SD	5.5 ± 3.7	2.8 ± 1.4	.03
Median	4.4	2.4	
Minimum	2.8	1.4	
Maximum	12.7	5.5	